2.E

Nuclear Physics **21** (1960) 256—269; © *North-Holland Publishing Co., Amsterdam*

A MODEL FOR THE CALCULATION OF THE OPTICAL POTENTIAL IN SOME FINITE NUCLEI

B. JANCOVICI

Laboratoire de Physique Théorique et Hautes Énergies, Faculté des Sciences, Orsay (S. et O.), France †

Received 12 July 1960

Abstract: The present paper describes in sect. 2 an explicit calculation of the optical potential, up to the second order in perturbations, in a simple model for the finite nuclei He^4, O^{16}, Ca^{40}, which are pictured as made of nucleons bound in an harmonic oscillator average potential; finite nucleus wave functions are used through the whole calculation, and no results pertinent to the infinite nuclear matter case are used. Numerical results for the imaginary potential are presented in sect. 3. Although our model is very crude, it is interesting to compare the results to those obtained through the Thomas-Fermi approximation, if only to test this approximation: this is done in sect. 4, where the conclusions are stressed. It is found that the imaginary potential at low energy has a maximum in the surface, a conclusion which had been previously derived only in the frame of the Thomas-Fermi approximation.

1. Introduction

The optical potential which describes the propagation of a neutron through infinite nuclear matter has been computed from two-body nucleon-nucleon forces [1]). All numerical studies in the case of finite nuclei [2–5]) use an approximation in which the optical potential, at a point with a given nuclear density, is taken equal to the optical potential in infinite nuclear matter of the same density; this approximation may be called the Thomas-Fermi approximation [2]).

Exact expansions of the optical potential in series of the two-body interaction have been given for finite nuclei [6–7]) and are represented by diagrams [8]). It seems, incidentally, that the prescription for computing the optical potential is not unique, because several potentials are able to reproduce the same elastic scattering amplitudes at a given energy. We anyhow replace in zeroth order the target nucleus by a one-body potential, U; the individual-particle model states are the bound and unbound eigenfunctions of this potential. Up to the second order, the optical potential $\mathscr{V}$ is then given by the diagrams of fig. 1, where the horizontal dotted line represents the two-body interaction v, and where the full lines are particle and holes; the target nucleus model state, which is assumed to be non-degenerate, is taken as the vacuum. These diagrams are to be interpreted as matrix elements of the optical potential between one-particle eigenstates of the zeroth-order potential U. Following the prescription of Bell and Squires [6]),

† Work supported in part by the United States Air Force through the European Office, Air Research and Development Command.

we consider the matrix elements between all occupied and unoccupied eigenstates.

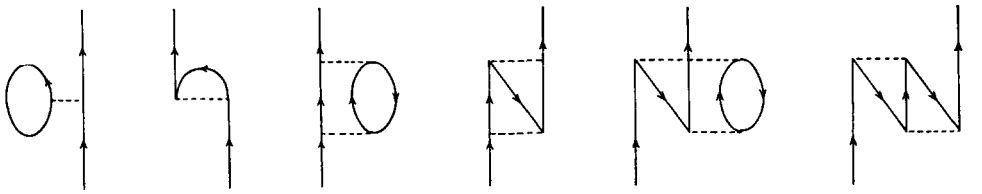

Fig. 1. The first and second order diagrams for the optical potential.

The optical potential which results from the graphs of fig. 1 is a non-local potential $\mathscr{V}(x_1, x_2)$ in coordinate space. We assume that the two-body interaction between two nucleons at points $\mathbf{x}_1$ and $\mathbf{y}_1$ is $\mathcal{O}v(\mathbf{x}_1-\mathbf{y}_1)$, where $\mathcal{O}$ is a spin and isobaric spin dependent operator. We call P_σ and P_τ the spin and isobaric spin exchange operators; $k(\mathbf{x}_1)$, $p(\mathbf{x}_1)$, $q(\mathbf{x}_1)$ are space eigenfunctions of the average potential $U(\mathbf{x}_1)$ and E_k, E_p, E_q are the corresponding energies. With these notations, the contributions of the graphs of fig. 1 are the following †:

$$\mathscr{V}^{(1a)}(\mathbf{x}_1, \mathbf{x}_2) = \tfrac{1}{4}\,\mathrm{Tr}\,\mathcal{O}\sum_{k<}\int k^*(\mathbf{y}_1)v(\mathbf{x}_1-\mathbf{y}_1)k(\mathbf{y}_1)\mathrm{d}\mathbf{y}_1\delta(\mathbf{x}_2-\mathbf{x}_1) \quad (1.1a)$$

($k <$ under the summation sign indicates that this summation runs on all occupied space states k; $>$ would mean a summation on unoccupied states),

$$\mathscr{V}^{(1b)}(\mathbf{x}_1, \mathbf{x}_2) = -\tfrac{1}{4}\,\mathrm{Tr}\,\mathcal{O}P_\sigma P_\tau \sum_{k<} k^*(\mathbf{x}_1)v(\mathbf{x}_1-\mathbf{x}_2)k(\mathbf{x}_2), \quad (1.1b)$$

$$\mathscr{V}^{(2a)}(\mathbf{x}_1, \mathbf{x}_2) = \tfrac{1}{4}\,\mathrm{Tr}\,\mathcal{O}^2$$

$$\times \sum_{\substack{k< \\ p,\,q>}} \frac{\int k^*(\mathbf{y}_2)v(\mathbf{x}_2-\mathbf{y}_2)p(\mathbf{x}_2)q(\mathbf{y}_2)\mathrm{d}\mathbf{y}_2\int p^*(\mathbf{x}_1)q^*(\mathbf{y}_1)v(\mathbf{x}_1-\mathbf{y}_1)k(\mathbf{y}_1)\mathrm{d}\mathbf{y}_1}{E+E_k-E_q-E_p} \quad (1.2a)$$

(E is the energy of the incident particle),

$$\mathscr{V}^{(2b)}(\mathbf{x}_1, \mathbf{x}_2) = -\tfrac{1}{4}\,\mathrm{Tr}\,\mathcal{O}^2P_\sigma P_\tau$$

$$\times \sum_{\substack{k< \\ p,\,q>}} \frac{\int k^*(\mathbf{y}_2)v(\mathbf{x}_2-\mathbf{y}_2)p(\mathbf{y}_2)q(\mathbf{x}_2)\mathrm{d}\mathbf{y}_2\int p^*(\mathbf{x}_1)q^*(\mathbf{y}_1)v(\mathbf{x}_1-\mathbf{y}_1)k(\mathbf{y}_1)\mathrm{d}\mathbf{y}_1}{E+E_k-E_p-E_q}, \quad (1.2b)$$

$$\mathscr{V}^{(2c)}(\mathbf{x}_1, \mathbf{x}_2) = \tfrac{1}{4}\,\mathrm{Tr}\,\mathcal{O}^2$$

$$\times \sum_{\substack{k,\,p< \\ q>}} \frac{\int p^*(\mathbf{x}_2)k^*(\mathbf{y}_2)v(\mathbf{x}_2-\mathbf{y}_2)q(\mathbf{y}_2)\mathrm{d}\mathbf{y}_2\int q^*(\mathbf{y}_1)v(\mathbf{x}_1-\mathbf{y}_1)p(\mathbf{x}_1)k(\mathbf{y}_1)\mathrm{d}\mathbf{y}_1}{E-E_k-E_p+E_q}, \quad (1.2c)$$

† The traces are meant on spin and isobaric spin states of two particles; Tr 1 = 16.

$$\mathscr{V}^{(2d)}(\mathbf{x}_1, \mathbf{x}_2) = -\tfrac{1}{4} \operatorname{Tr} \mathcal{O}^2 P_\sigma P_\tau$$

$$\times \sum_{\substack{k, p< \\ q>}} \frac{\int p^*(\mathbf{x}_2) k^*(\mathbf{y}_2) v(\mathbf{x}_2 - \mathbf{y}_2) q(\mathbf{y}_2) d\mathbf{y}_2 \int q^*(\mathbf{y}_1) v(\mathbf{x}_1 - \mathbf{y}_1) p(\mathbf{y}_1) k(\mathbf{x}_1) d\mathbf{y}_1}{E - E_k - E_p + E_q}. \quad (1.2d)$$

In the cases (1.2a) and (1.2b) where the energy denominator may vanish, the energy E must have an imaginary part, the result of which will be to perform an average on the resonances [9]; as a consequence (1.2a) and (1.2b) will contribute an imaginary part to the optical potential. Our main interest in the present paper will actually be the imaginary part, for two reasons:

a) The leading term for the real part (1.1a) is a local potential identical to the result of the Thomas-Fermi approximation. On the contrary, the leading terms for the imaginary part are second order graphs, and they are rather different in their structure from the Thomas-Fermi analogous terms. Therefore the finite size of the nucleus, if it has any effect, will mostly be apparent in the imaginary part.

b) The practical computation of the second-order terms is faster for their imaginary part because the imaginary parts of the series (1.2a) and (1.2b) converge more quickly.

We shall now proceed to the actual calculation of this imaginary potential in a simple model.

2. Calculations in the Harmonic Oscillator Model

For actual computations, we shall from now on assume that the average potential U is a harmonic oscillator potential

$$U(\mathbf{x}_1) = \frac{\hbar^2 \nu^2}{2M} x_1^2 \quad (2.1)$$

($\hbar$ is the Planck constant, M the nucleon mass and ν a parameter which decribes the strength of U). Of course, strictly speaking, we are interested in a scattering problem and we would need a zeroth order potential U going to zero at infinity. It would be more correct to say that what we do is to approximate these bound and unbound eigenfunctions and eigenvalues which explicitly appear in (1.1) and (1.2) by those ones of a harmonic oscillator. This is of course a rather crude model, but its comparison with the extreme opposite case of infinite nuclear matter could be of interest.

We furthermore assume that the two-body interaction is gaussian:

$$\mathcal{O}v(\mathbf{x}_1 - \mathbf{y}_1) = \mathcal{O}\Lambda e^{-\alpha^2(\mathbf{x}_1 - \mathbf{y}_1)^2} \quad (2.2)$$

and it is then rather convenient to perform all calculations with the relative and centre-of-mass variables

$$\mathbf{x}_2 - \mathbf{x}_1 = \mathbf{x}, \quad \mathbf{x}_2 + \mathbf{x}_1 = 2\mathbf{X}, \quad \mathbf{y}_2 - \mathbf{y}_1 = \mathbf{y}, \quad \mathbf{y}_2 + \mathbf{y}_1 = 2\mathbf{Y}. \quad (2.3)$$

With these variables, it is shown in the Appendix that a partial summation on one harmonic oscillator shell can be carried for the contribution of this shell to the mixed density function

$$D_n(Y, y) \equiv \sum_{\substack{k \\ E_k = E_n}} k^*(\mathbf{y}_2)k(\mathbf{y}_1) = \left(\frac{\nu}{\pi}\right)^{\frac{3}{2}} \mathrm{e}^{-\frac{1}{2}\nu(2Y^2+\frac{1}{2}y^2)} \mathscr{L}_n(Y, y), \tag{2.4}$$

where

$$\mathscr{L}_n(Y, y) = \sum_{h=0}^{n} (-)^h L_h^{(\frac{1}{2})}(2\nu Y^2) L_{n-h}^{(\frac{1}{2})}(\tfrac{1}{2}\nu y^2) \tag{2.5}$$

($L_h^{(\frac{1}{2})}$ denotes a Laguerre associated polynomial [10]). This function D_n happens to depend only on the lengths of $\mathbf{Y}$ and $\mathbf{y}$.

Explicit expressions can then easily be obtained for the first-order contributions (1.1a) and (1.1b). The computation of the second-order contributions is much simplified by adopting the same two-body interaction parameters in (2.2) as in the work of Verlet [1]) on infinite nuclear matter: the exchange dependence $\mathcal{O}$ is such that $\mathrm{Tr}\, \mathcal{O}^2 P_\sigma P_\tau$ vanishes, and so there are no contributions from (1.2b) and (1.2d). The remaining contributions, which are the only ones for which the computation is not trivial, are (1.2a) and (1.2c); (1.2a) is especially important since it is here the only contribution to the imaginary part of the optical potential, due to the imaginary part of E in the denominator.

The product of two-body interactions which appears in (1.2a) and (1.2c) is easily seen to be

$$v(\mathbf{x}_2 - \mathbf{y}_2)v(\mathbf{x}_1 - \mathbf{y}_1) = \Lambda^2 \mathrm{e}^{-\alpha^2[2(\mathbf{X}-\mathbf{Y})^2 + \frac{1}{2}(\mathbf{x}-\mathbf{y})^2]} \tag{2.6}$$

and, from (2.4), (1.2a) becomes

$$\mathscr{V}^{(2a)} = \frac{\mathrm{Tr}\, \mathcal{O}^2 \Lambda^2}{4\hbar\omega} \left(\frac{\nu}{\pi}\right)^{\frac{3}{2}} \mathrm{e}^{-\frac{1}{2}\nu(2X^2+\frac{1}{2}x^2)}$$

$$\times \sum_{\substack{n< \\ m,\, l>}} \frac{\mathscr{L}_l(X, x) \iint \mathrm{e}^{-2\alpha^2(\mathbf{X}-\mathbf{Y})^2 - \frac{1}{2}\alpha^2(\mathbf{x}-\mathbf{y})^2 - \nu(2Y^2+\frac{1}{2}y^2)} \mathscr{L}_n(Y, y)\mathscr{L}_m(Y, y) \mathrm{d}\mathbf{Y}\, \mathrm{d}\mathbf{y}}{\varepsilon + ij - \frac{3}{2} + n - m - l}, \tag{2.7}$$

where the index n runs on all occupied shells ($n = 0, 1, \ldots$), and the indices m and l, on all empty shells. $\varepsilon + ij$ is the energy in units of $\hbar\omega = \hbar\nu/M$ with a small averaging part j; ε is measured from the bottom of the well.

A similar expression, but with no imaginary part, could be given for (1.2c); the only difference would be in a summation on n, l $\langle$and $m\rangle$, and in an $\varepsilon - \frac{3}{2} - n - l + m$ in the denominator.

For further calculations, we shall now specialize to given nuclei, and obtain numerical values for the imaginary part of (2.7).

2.1. He^4

In the case of He^4 only one shell ($n = 0$) is occupied; for that shell $\mathscr{L}_0 = 1$, and we obtain from (2.7)

$$\mathscr{V}^{(2a)} = \frac{\mathrm{Tr}\,\mathscr{O}^2\Lambda^2}{4\hbar\omega}\left(\frac{\nu}{\pi}\right)^{\frac{3}{2}} e^{-\frac{1}{2}\nu(2X^2+\frac{1}{2}x^2)} \times \sum_{m,\,l=1}^{\infty} \frac{\mathscr{L}_l(X,x)\iint e^{-2\alpha^2(\mathbf{X}-\mathbf{Y})^2-\frac{1}{2}\alpha^2(\mathbf{x}-\mathbf{y})^2-\nu(2Y^2+\frac{1}{2}y^2)}\mathscr{L}_m(Y,y)\mathrm{d}\mathbf{Y}\,\mathrm{d}\mathbf{y}}{\varepsilon+ij-\frac{3}{2}-m-l}. \quad (2.8)$$

Using (2.6), we see that the double integral in (2.8) is a sum of products of integrals [11]) like for instance

$$\int e^{-2(\alpha^2+\nu)Y^2+4\alpha^2\mathbf{X}\cdot\mathbf{Y}} L_h^{(\frac{1}{2})}(2\nu Y^2)\mathrm{d}\mathbf{Y} = 4\pi\int_0^\infty e^{-2(\alpha^2+\nu)Y^2}\frac{\sinh 4\alpha^2 XY}{4\alpha^2 XY} L_h^{(\frac{1}{2})}(2\nu Y^2)Y^2\mathrm{d}Y \quad (2.9)$$

$$= \left(\frac{\pi}{2(\alpha^2+\nu)}\right)^{\frac{3}{2}}\left(\frac{\alpha^2}{\alpha^2+\nu}\right)^h e^{\frac{2\alpha^4}{\alpha^2+\nu}X^2} L_h^{(\frac{1}{2})}\left(\frac{\alpha^2}{\alpha^2+\nu}2\nu X^2\right),$$

and we obtain for (2.8)

$$\mathscr{V}^{(2a)}(X,x) = \frac{\mathrm{Tr}\,\mathscr{O}^2\Lambda^2}{4\hbar\omega}\left(\frac{\nu}{\pi}\right)^{\frac{3}{2}}\left(\frac{\nu}{\alpha^2+\nu}\right)^3 e^{-\frac{(3\alpha^2+\nu)\nu}{2(\alpha^2+\nu)}(2X^2+\frac{1}{2}x^2)} \times \sum_{m,\,l=1}^{\infty} \frac{\mathscr{L}_l(X,x;1)\,\mathscr{L}_m\left(X,x;\frac{\alpha^2}{\alpha^2+\nu}\right)\left(\frac{\alpha^2}{\alpha^2+\nu}\right)^m}{\varepsilon+ij-\frac{3}{2}-m-l}, \quad (2.10)$$

where

$$\mathscr{L}_m(X,x;t) = \sum_{h=0}^{m}(-)^h L_h^{(\frac{1}{2})}(t2\nu X^2) L_{m-h}^{(\frac{1}{2})}\left(t\frac{\nu}{2}x^2\right), \quad (2.11)$$

and therefore

$$\mathscr{L}_m(X,x;1) \equiv \mathscr{L}_m(X,x). \quad (2.12)$$

2.2. O^{16}

Two shells ($n = 0, 1$) are now occupied, the contributions of which to (2.7) will be called $\mathscr{V}_0^{(2a)}$ and $\mathscr{V}_1^{(2a)}$:

$$\mathscr{V}^{(2a)} = \mathscr{V}_0^{(2a)} + \mathscr{V}_1^{(2a)}. \quad (2.13)$$

$\mathscr{V}_0^{(2a)}$ is given by (2.10), with the modification that m and l now run from 2 to ∞.

$\mathscr{V}_1^{(2a)}$ is the term of (2.7) with $n = 1$; using

$$\mathscr{L}_1(Y,y) = 2\nu Y^2 - \tfrac{1}{2}\nu y^2, \quad (2.14)$$

and the relation [10])

$$xL_n^{(\frac{1}{2})}(x) = -(n+1)L_{n+1}^{(\frac{1}{2})}(x)+(2n+\tfrac{3}{2})L_n^{(\frac{1}{2})}(x)-(n+\tfrac{1}{2})L_{n-1}^{(\frac{1}{2})}(x), \quad (2.15)$$

one obtains

$$\mathscr{L}_1(Y,y)\mathscr{L}_m(Y,y) = (m+1)\mathscr{L}_{m+1}(Y,y)+2\mathscr{M}_m(Y,y)+(m+2)\mathscr{L}_{m-1}(Y,y), \quad (2.16)$$

where

$$\mathscr{M}_m(Y,y) = \sum_{h=0}^{m}(-)^h(2h-m)L_h^{(\frac{1}{2})}(2\nu Y^2)L_{m-h}^{(\frac{1}{2})}\left(\frac{\nu}{2}y^2\right). \quad (2.17)$$

Using (2.16) in (2.7), and performing the integrals with the help of (2.9), one obtains

$$\mathscr{V}_1^{(2a)}(X,x) = \frac{\mathrm{Tr}\,\mathcal{O}^2\Lambda^2}{4\hbar\omega}\left(\frac{\nu}{\pi}\right)^{\frac{3}{2}}\left(\frac{\nu}{\alpha^2+\nu}\right)^3 e^{-\frac{(3\alpha^2+\nu)\nu}{2(\alpha^2+\nu)}(2X^2+\frac{1}{2}x^2)}$$

$$\times\sum_{m,\,l=2}^{\infty}\frac{\mathscr{L}_l(X,x;1)}{\varepsilon+ij-\frac{1}{2}-m-l}\left[(m+1)\mathscr{L}_{m+1}\left(X,x;\frac{\alpha^2}{\alpha^2+\nu}\right)\left(\frac{\alpha^2}{\alpha^2+\nu}\right)^{m+1}\right. \quad (2.18)$$

$$\left.+2\mathscr{M}_m\left(X,x;\frac{\alpha^2}{\alpha^2+\nu}\right)\left(\frac{\alpha^2}{\alpha^2+\nu}\right)^m+(m+2)\mathscr{L}_{m-1}\left(X,x;\frac{\alpha^2}{\alpha^2+\nu}\right)\left(\frac{\alpha^2}{\alpha^2+\nu}\right)^{m-1}\right],$$

where

$$\mathscr{M}_m(X,x;t) = \sum_{h=0}^{m}(-)^h(2h-m)L_h^{(\frac{1}{2})}(t2\nu X^2)L_{m-h}^{(\frac{1}{2})}\left(t\frac{\nu}{2}x^2\right). \quad (2.19)$$

2.3. Ca^{40}

Three shells ($n = 0, 1, 2$) are now occupied, the contribution of which to (7) will be called $\mathscr{V}_0^{(2a)}$, $\mathscr{V}_1^{(2a)}$, and $\mathscr{V}_2^{(2a)}$:

$$\mathscr{V}^{(2a)} = \mathscr{V}_0^{(2a)}+\mathscr{V}_1^{(2a)}+\mathscr{V}_2^{(2a)}. \quad (2.20)$$

$\mathscr{V}_0^{(2a)}$ is given by (2.10), with the modification that m and l now run from 3 to ∞; similarly $\mathscr{V}_1^{(2a)}$ is given by (2.18) with the same modification.

$\mathscr{V}_2^{(2a)}$ is the term of (2.7) with $n = 2$; using

$$\mathscr{L}_2(Y,y) = \tfrac{3}{2}-\tfrac{1}{2}\nu y^2-2\nu Y^2+\tfrac{1}{2}(\tfrac{1}{2}\nu y^2)^2-\tfrac{1}{2}\nu y^2 2\nu Y^2+\tfrac{1}{2}(2\nu Y^2)^2, \quad (2.21)$$

and the relation (2.15), one obtains

$$\mathscr{L}_2(Y,y)\mathscr{L}_m(Y,y) = \tfrac{1}{2}(m^2+3m+2)\mathscr{L}_{m+2}(Y,y)+2m\mathscr{M}_{m+1}(Y,y)$$
$$+m(m+1)\mathscr{L}_m(Y,y)+2\mathscr{N}_m(Y,y) \quad (2.22)$$
$$+2(m+2)\mathscr{M}_{m-1}(Y,y)+\tfrac{1}{2}(m^2+3m+2)\mathscr{L}_{m-2}(Y,y),$$

where

$$\mathscr{N}_m(Y, y) = \sum_{h=0}^{m} (-)^h (2h-m)^2 L_h^{(\frac{1}{2})}(2\nu Y^2) L_{m-h}^{(\frac{1}{2})}\left(\frac{\nu}{2} y^2\right). \tag{2.23}$$

Using (2.22) in (2.7), and performing the integrals with the help of (2.9), one obtains

$$\begin{aligned}
\mathscr{V}_2^{(2a)}(X, x) = {} & \frac{\mathrm{Tr}\, \mathscr{O}^2 \Lambda^2}{4\hbar\omega} \left(\frac{\nu}{\pi}\right)^{\frac{3}{2}} \left(\frac{\nu}{\alpha^2+\nu}\right)^3 \mathrm{e}^{-\frac{(3\alpha^2+\nu)\nu}{2(\alpha^2+\nu)}(2X^2+\frac{1}{2}x^2)} \\
& \times \sum_{m,\, l=3}^{\infty} \frac{\mathscr{L}_l(X, x;\, 1)}{\varepsilon + ij + \frac{1}{2} - m - l} \left\{ \tfrac{1}{2}(m+2)(m+1) \mathscr{L}_{m+2}\left(X, x; \frac{\alpha^2}{\alpha^2+\nu}\right)\left(\frac{\alpha^2}{\alpha^2+\nu}\right)^{m+2} \right. \\
& + 2m \mathscr{M}_{m+1}\left(X, x; \frac{\alpha^2}{\alpha^2+\nu}\right)\left(\frac{\alpha^2}{\alpha^2+\nu}\right)^{m+1} \\
& + \left[m(m+1) \mathscr{L}_m\left(X, x; \frac{\alpha^2}{\alpha^2+\nu}\right) + 2\mathscr{N}_m\left(X, x; \frac{\alpha^2}{\alpha^2+\nu}\right) \right] \left(\frac{\alpha^2}{\alpha^2+\nu}\right)^m \\
& + 2(m+2) \mathscr{M}_{m-1}\left(X, x; \frac{\alpha^2}{\alpha^2+\nu}\right)\left(\frac{\alpha^2}{\alpha^2+\nu}\right)^{m-1} \\
& \left. + \tfrac{1}{2}(m+2)(m+1) \mathscr{L}_{m-2}\left(X, x; \frac{\alpha^2}{\alpha^2+\nu}\right)\left(\frac{\alpha^2}{\alpha^2+\nu}\right)^{m-2} \right\},
\end{aligned} \tag{2.24}$$

where

$$\mathscr{N}_m(X, x; t) = \sum_{h=0}^{m} (-)^h (2h-m)^2 L_h^{(\frac{1}{2})}(t 2\nu X^2) L_{m-h}^{(\frac{1}{2})}\left(t \frac{\nu}{2} x^2\right). \tag{2.25}$$

3. Numerical Calculations

The Laguerre polynomials, the functions (2.11), (2.19) and (2.25), and finally the imaginary part of the double series (2.10), (2.18) and (2.24) were evaluated for different values of the variables, using an IBM 650 digital computer.

The value of the harmonic oscillator parameter was adjusted for each nucleus to fit the measured mean square radius [12]), taking into account the centre-of-mass motion [13]). These parameters and those ones of the two-body potential [1]) are listed in table 1.

TABLE 1

The numerical constants

$\alpha = 0.674\, f^{-1}$ ($f = 10^{-13}$ cm), $\Lambda = 72$ MeV, $\mathrm{Tr}\, \mathscr{O}^2 = 8.54$		
He^4	$\nu = 0.463\, f^{-1}$	$\hbar\omega = 19.1$ MeV
O^{16}	$\nu = 0.338\, f^{-1}$	$\hbar\omega = 14.0$ MeV
Ca^{40}	$\nu = 0.242\, f^{-1}$	$\hbar\omega = 10.0$ MeV

The averaging parameter j

In the case of He^4, Im $\mathscr{V}^{(2a)}(0, 0)$ was first computed as a function of the energy $\varepsilon\hbar\omega$ for 3 values $j = 1, 2, 3$ of the averaging parameter. The curves of fig. 2 show how the oscillations of Im $\mathscr{V}^{(2a)}$ are damped when j increases, since

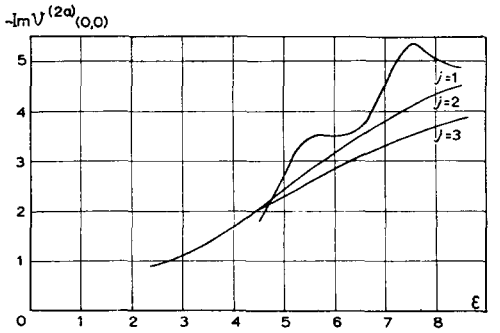

Fig. 2. $(He^4) - \text{Im } \mathscr{V}^{(2a)}(0, 0)$ in MeV/f^3 as a function of ε for different values of j ($f = 10^{-13}$ cm). ε is in units of $\hbar\omega = 19.1$ MeV.

the effect of j is to average $\mathscr{V}^{(2a)}$ over an energy interval of the order of $j\hbar\omega$. It is seen that a reasonable damping is obtained for $j \geqq 2$, and the value $j = 2$ will be used in all further calculations.

He^4

The non-local imaginary potential Im $\mathscr{V}^{(2a)}(X, x)$ depends on X and x as defined by (2.3). The values 'at the centre of the nucleus' are obtained for $X = 0$, and the dependence on x then shows the non-local extension of the potential. This function Im $\mathscr{V}^{(2a)}(0, x)$ is plotted on fig. 3 for several values of

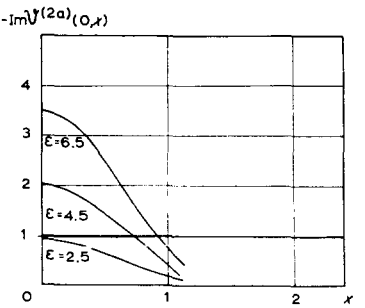

Fig. 3. $(He^4) - \text{Im } \mathscr{V}^{(2a)}(0, x)$ in MeV/f^3 as a function of x (in units of f) for different values of ε.

the energy. It is seen that the range of the non-locality (the value of x at which Im $\mathscr{V}^{(2a)}$ is half of its value at $x = 0$) is about 0.6 or $0.7f$ ($f = 10^{-13}$ cm).

An 'equivalent local potential' can be defined by

$$\mathscr{V}_{\mathrm{loc}}(X) = 4\pi \int_0^\infty \mathscr{V}(X, x)x^2 \mathrm{d}x \tag{3.1}$$

Im $\mathscr{V}_{\mathrm{loc}}(0)$ is plotted on fig. 4 as a function of the energy.

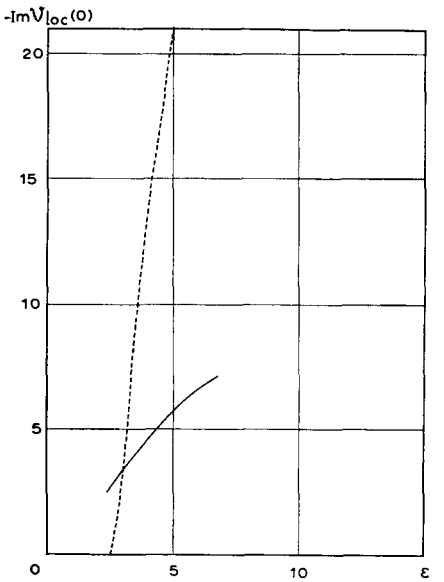

Fig. 4. (He^4) — Im $\mathscr{V}_{\mathrm{loc}}(0)$ in MeV as a function of ε. ε is in units of $\hbar\omega = 19.1$ MeV. The dotted line is the Thomas-Fermi approximation.

O^{16}

Im $\mathscr{V}^{(2a)}(0, x)$ is plotted on fig. 5 and Im $\mathscr{V}_{\mathrm{loc}}(0)$ on fig. 6. It is seen that the range of the non-locality is about $0.9f$.

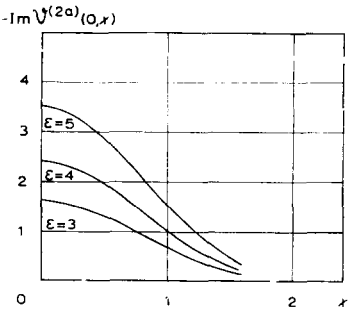

Fig. 5. (O^{16}) — Im $\mathscr{V}^{(2a)}(0, x)$ in MeV/f^3 as a function of x (in units of f) for different values of ε.

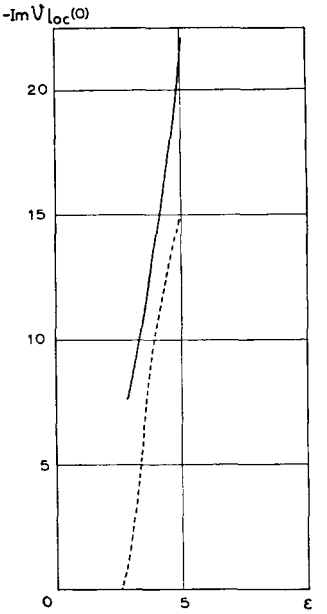

Fig. 6. $(O^{16}) - \mathrm{Im}\ \mathscr{V}_{\mathrm{loc}}(0)$ in MeV as a function of ε. ε is in units of $\hbar\omega = 14$ MeV. The dotted line is the Thomas-Fermi approximation.

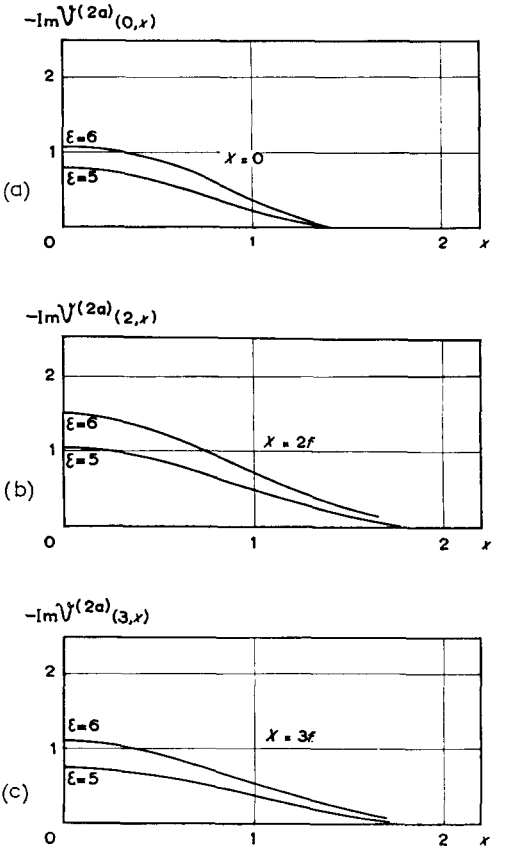

Fig. 7. $(Ca^{40}) - \mathrm{Im}\ \mathscr{V}^{(2a)}(X, x)$ in MeV/f^3 as a function of x (in units of f) for different values of ε and X.

Ca^{40}

Im $\mathscr{V}^{(2a)}(X, x)$ is plotted on fig. 7 for the values $X = 0, 2, 3f$ respectively. It is seen that the range of the non-locality increases with X, from about $0.8f$ for $X = 0$ to $1f$ for $X = 3$. The depth also varies with a maximum at $X = 2$. As a result, the imaginary equivalent local potential Im $\mathscr{V}_{loc}(X)$, which is plotted on fig. 8 as a function of X, shows a variation with X and it has a maximum around $X = 2$. The suggestion that the absorbtive potential has a maximum in the surface is once more supported.

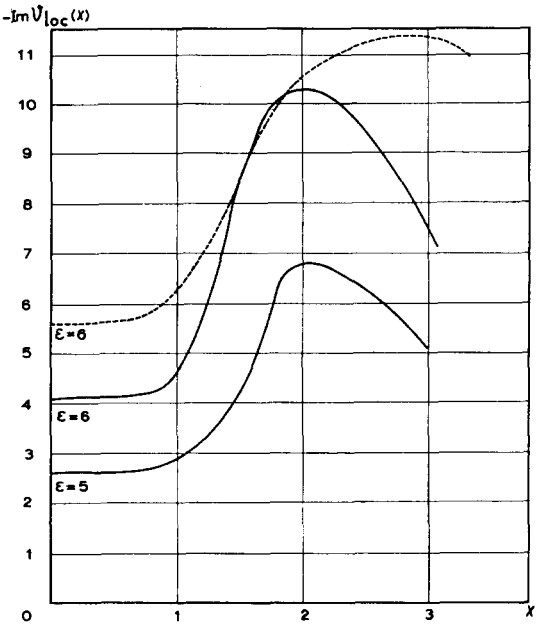

Fig. 8. (Ca^{40}) — Im $\mathscr{V}_{loc}(X)$ in MeV as a function of X (in units of f) for two different values of ε. The dotted line is the Thomas-Fermi approximation.

4. Discussion

We do not intend to carry on here a detailed comparison of our results with the experimental information. We do not look for any qualitative agreement, due to the crudeness of our model. For instance, we know that the convergence of the perturbation expansion is very poor [2]). Furthermore, to our knowledge, there are no available analyses of experiments on the basis of a non-local imaginary potential †. We, however, suggest that such analyses should be made; the rough estimate of the present paper is a non-locality 'range' of about 0.8 to $1f$.

It is more interesting to compare the imaginary equivalent local potential of the present calculation with the results of the Thomas Fermi approximation

† *Note added in proof:* Such an analysis has appeared after the present paper was submitted for publication [14]).

as used by Verlet [1]). (Incidentally, these results are themselves in fair agreement with experiment). To make the comparison precise, we define at each point X a local Fermi momentum k_0 which is related to the density $\rho(X)$ at this point by the customary relation for an infinite medium

$$\rho(X) = (16/3\pi^2)k_0^3; \tag{4.1}$$

we also define an incident particle momentum in the well k_N by the relation

$$\varepsilon\hbar\omega = k_N^2/2M. \tag{4.2}$$

We then follow the prescriptions of Verlet for the second-order computation of Im $\mathscr{V}_{loc}(X)$ in infinite nuclear matter, with the above determined values of k_0 and k_N. The results of these calculations are plotted in dotted lines on figs. 4, 6, 8. Fig. 4 shows that He^4 is very poorly described by the Thomas-Fermi approximation, a not very surprising result for a nucleus in which only one space state is occupied. The agreement in the case of O^{16} (Fig. 6) can be considered as fair especially if we remember that the imaginary potential is a very sensitive function of the energy, and that the comparison of the energies between the two models is not obvious to define; the comparison is of course not significant when k_N goes to k_0 ($\varepsilon = 2.5$ in the case of O^{16}), because the Thomas-Fermi model then predicts a vanishing imaginary potential. For this reason, in the case of Ca^{40} (fig. 8), we have plotted the Thomas-Fermi curve only for the case $\varepsilon = 6$. The agreement between the shell model and the Thomas-Fermi approximation is then rather good; in the surface (for $X \approx 3f$), the Thomas-Fermi approximation overestimates the imaginary potential, but this is to be expected because this approximation probably overestimates the effect of the Pauli principle.

Our shell model calculation nevertheless shows that the absorption has a maximum in the surface; this very important effect is therefore not a spurious result of the Thomas-Fermi approximation, and this is the main conclusion of the present paper †.

The possible effect of the clusters in the surface is, however, not yet clarified.

The author is indebted to Miss E. Yeivine for her kind help in the programmation for the IBM 650 computer and to Dr. L. Verlet for interesting discussions.

Appendix

MIXED DENSITY FUNCTION FOR A CLOSED SHELL IN A HARMONIC OSCILLATOR POTENTIAL

We wish to compute the contribution from the nth harmonic oscillator shell ($n = 0, 1, 2 \ldots$) to the mixed density function, for particles in one spin and

† The stronger absorption in the surface would probably be even more enhanced in a calculation beyond the second order [2]).

isobaric spin state. This function is

$$D_n = \sum_{k \text{ in shell } n} k^*(\mathbf{r}_1)k(\mathbf{r}_2), \tag{A.1}$$

where k are the space wave functions. The quantity $k^*(\mathbf{r}_1)k(\mathbf{r}_2)$ may alternatively be thought of as the total wave function for two particles in the states k and k^*; it is well known that such a wave function may be expressed as a finite sum of products of a function of $\mathbf{R} = \frac{1}{2}(\mathbf{r}_1+\mathbf{r}_2)$ by a function of $\mathbf{r} = \mathbf{r}_2-\mathbf{r}_1$. We shall see that D_n is actually rather simple with these variables.

We first notice that

$$D_0 = (\nu/\pi)^{\frac{3}{4}} e^{-\frac{1}{2}\nu(r_1^2+r_2^2)} = (\nu/\pi)^{\frac{3}{4}} e^{-\frac{1}{4}\nu(2R^2+\frac{1}{2}r^2)}. \tag{A.2}$$

D_n for higher shells will now be obtained by the use of appropriate elevation operators. A state $k(\mathbf{r}_i)$ $(i = 1,2)$ of energy $(n+\frac{1}{2})\hbar\omega$ may be separated in cartesian coordinates x_i, y_i, z_i as

$$k(\mathbf{r}_i) = f_a(x_i)g_b(y_i)h_c(z_i), \tag{A.3}$$

where $(a+\frac{1}{2})\hbar\omega$ is, for instance, the energy for the x_i oscillation mode; of course

$$a+b+c = n. \tag{A.4}$$

$f_a(x_i)$ may be obtained from

$$f_0(x_i) = (\nu/\pi)^{\frac{1}{4}} e^{-(\frac{1}{2}\nu x_i^2)} \tag{A.5}$$

with the help of the elevation operator

$$\xi_i = (\tfrac{1}{2}\nu)^{\frac{1}{2}}(\nu x_i - \partial/\partial x_i); \tag{A.6}$$

one has

$$f_a(x_i) = \frac{1}{\sqrt{a!}} \xi_i^a f_0(x_i) \tag{A.7}$$

and similar equations for y_i and z_i with operators η_i and ζ_i respectively. Therefore

$$k(\mathbf{r}_i) = \frac{\xi_i^a \eta_i^b \zeta_i^c}{\sqrt{a!\,b!\,c!}} \left(\frac{\nu}{\pi}\right)^{\frac{3}{4}} e^{-\frac{1}{2}\nu r_i^2} \tag{A.8}$$

and (A.1) may be written

$$\begin{aligned} D_n &= \sum_{a+b+c=n} \frac{(\xi_2\xi_1)^a(\eta_2\eta_1)^b(\zeta_2\zeta_1)^c}{a!\,b!\,c!} D_0 = \frac{1}{n!}(\xi_2\xi_1+\eta_2\eta_1+\zeta_2\zeta_1)^n D_0 \\ &= \frac{1}{n!}(\boldsymbol{\varrho}_2 \cdot \boldsymbol{\varrho}_1)^n D_0, \end{aligned} \tag{A.9}$$

where

$$\boldsymbol{\varrho}_i = (\tfrac{1}{2}\nu)^{\frac{1}{2}}(\nu \mathbf{r}_i - \partial/\partial \mathbf{r}_i). \tag{A.10}$$

We can take the variables **R** and **r**; we obtain

$$\boldsymbol{\varrho}_1 = (1/\sqrt{2})(\mathbf{P}-\boldsymbol{\varrho}), \quad \boldsymbol{\varrho}_2 = (1/\sqrt{2})(\mathbf{P}+\boldsymbol{\varrho}), \tag{A.11}$$

where

$$\mathbf{P} = (\tfrac{1}{4}\nu)^{\frac{1}{2}}[2\nu\mathbf{R}-\partial/\partial\mathbf{R}], \quad \boldsymbol{\varrho} = (1/\nu)^{\frac{1}{2}}[\tfrac{1}{2}\nu\mathbf{r}-\partial/\partial\mathbf{r}], \tag{A.12}$$

and from (A.9) and (A.11)

$$D_n = \frac{1}{n!}\left(\frac{P^2-\rho^2}{2}\right)^n D_0. \tag{A.13}$$

Since **P** is an elevation operator in the **R** space, each term P^{2m} in the expansion of (A.13) must generate, from the factor $\exp(-\nu R^2)$ in D_0, the m^{th}s harmonic oscillator wave function (since P^2 is a scalar, only s states are obtained). These wave functions involve [10]) associated Laguerre polynomials $L_n^{(\frac{1}{2})}(2\nu R^2)$. More precisely, using the definition

$$L_n^{(\alpha)}(x) = \frac{\mathrm{e}^x x^{-\alpha}}{n!}\frac{\mathrm{d}^n}{\mathrm{d}x^n}(\mathrm{e}^{-x}x^{n+\alpha}), \tag{A.14}$$

it can be shown that

$$P^2\mathrm{e}^{-\nu R^2}L_{n-1}^{(\frac{1}{2})}(2\nu R^2) = -2n\mathrm{e}^{-\nu R^2}L_n^{(\frac{1}{2})}(2\nu R^2) \tag{A.15}$$

and similarly

$$\rho^2\mathrm{e}^{-\frac{1}{2}\nu r^2}L_{n-1}^{(\frac{1}{2})}(\tfrac{1}{2}\nu r^2) = -2n\mathrm{e}^{-\frac{1}{2}\nu r^2}L_n^{(\frac{1}{2})}(\tfrac{1}{2}\nu r^2); \tag{A.15'}$$

(A.13) then becomes

$$D_n = (\nu/\pi)^{\frac{3}{4}}\mathrm{e}^{-\frac{1}{2}\nu(2R^2+\frac{1}{2}r^2)}\sum_{h=0}^{n}(-)^h L_h^{(\frac{1}{2})}(2\nu R^2)L_{n-h}^{(\frac{1}{2})}(\tfrac{1}{2}\nu r^2). \tag{A.16}$$

It is interesting to notice that D_n does not depend on the angle between **R** and **r**.

References

1) L. Verlet, Nuovo Cim. **7** (1958) 821; Ann. de Phys. **4** (1959) 643. (Earlier references are given there)
2) L. Verlet and J. Gavoret, Nuovo Cim. **10** (1958) 505
3) K. Harada and N. Oda, Prog. Theor. Phys. **21** (1959) 260
4) G. L. Shaw, Ann. of Phys. **8** (1959) 509
5) L. C. Gomes, Phys. Rev. **116** (1959) 1226
6) J. S. Bell and E. J. Squires, Phys. Rev. Letters **3** (1959) 96
7) L. M. Frantz and R. T. Mills, Nuclear Physics **15** (1960) 16
8) J. Goldstone, Proc. Roy. Soc. A **239** (1957) 267
9) G. E. Brown, C. J. De Dominicis and J. S. Langer, Ann. of Physics **6** (1959) 209
10) W. Magnus and F. Oberhettinger, Formulas and theorems for the functions of mathematical physics (Chelsea Publishing Co., 1954) p. 84
11) A. Erdélyi *et al.*, Tables of Integral Transforms (Mc Graw Hill, 1954), vol. II, p. 43
12) D. G. Ravenhall, Rev. Mod. Phys. **30** (1958) 430
13) L. J. Tassie and F. C. Barker, Phys. Rev. **111** (1958) 940
14) Wyatt, Wills and Green, Phys. Rev. **119** (1960) 1031